Ann. Geophys., 37, 289–297, 2019
https://doi.org/10.5194/angeo-37-289-2019
© Author(s) 2019. This work is distributed under
the Creative Commons Attribution 4.0 License.

Annales Geophysicae Open Access EGU

Magnetic dipolarizations inside geosynchronous orbit with tailward ion flows

Xiaoying Sun[1,2], **Weining William Liu**[1], **and Suping Duan**[1]

[1]State Key Laboratory of Space Weather, National Space Science Center (NSSC), Chinese Academy of Sciences (CAS), Beijing, 100190, China
[2]University of Chinese Academy of Sciences, Beijing, 100049, China

Correspondence: Weining William Liu (wliu@nssc.ac.cn) and Suping Duan (spduan@nssc.ac.cn)

Received: 19 November 2018 – Discussion started: 22 November 2018
Accepted: 10 April 2019 – Published: 6 May 2019

Abstract. Electromagnetic field and plasma data from the Time History of Events and Macroscale Interactions during Substorms (THEMIS) near-Earth probes are used to investigate magnetic dipolarizations inside geosynchronous orbit on 27 August 2014 during an intense substorm with $AE_{max} \sim 1000$ nT. THEMIS-D (TH-D) was located inside geosynchronous orbit around midnight in the interval from 09:25 to 09:55 UT. During this period, two distinct magnetic dipolarizations with tailward ion flows are observed by TH-D. The first one is indicated by the magnetic elevation angle increase from 15 to 25° around 09:30:40 UT. The tailward perpendicular velocity is $V_{\perp x} \sim -50\,km\,s^{-1}$. The second one is presented by the elevation angle increase from 25 to 45° around 09:36 UT, and the tailward perpendicular velocity is $V_{\perp x} \sim -70\,km\,s^{-1}$. These two significant dipolarizations are accompanied with the sharp increase in the energy flux of energetic electron inside geosynchronous orbit. After a 5 min expansion of the near-Earth plasma sheet (NEPS), THEMIS-E (TH-E) located outside geosynchronous orbit also detected this tailward expanding plasma sheet with ion flows of $-150\,km\,s^{-1}$. The dipolarization propagates tailward with a speed of $-47\,km\,s^{-1}$ along a 2.2 R_E distance in the X direction between TH-D and TH-E within 5 min. These dipolarizations with tailward ion flows observed inside geosynchronous orbit indicate a new energy transfer path in the inner magnetosphere during substorms.

1 Introduction

Magnetic dipolarization can be observed at or inside geosynchronous orbit during intense substorms with high Auroral Electrojet (AE) indices (AE > 500 nT) (e.g., Dai et al., 2015; Nagai, 1982; Nosé et al., 2014; Ohtani et al., 2018). Dipolarizations are marked by the magnetic elevation angle increase with the decrease in the radial components of B_x and B_y and the increase in the B_z component (Liu and Liang, 2009; Duan et al., 2011; Dai et al., 2014, 2015). Ohtani et al. (2018) presented the statistical characteristics of magnetic dipolarizations inside geosynchronous orbit. They reported that the dipolarization region expanded in the azimuthal direction with a speed of $60\,km\,s^{-1}$ at 5.5 R_E. Using multiple satellite conjunction observations at or inside geosynchronous orbit, Dai et al. (2015) reported that the large dipolarization electric field was associated with a substorm injection of MeV electrons into the inner magnetosphere ($r < 6.6\,R_E$).

Magnetic dipolarizations are accompanied with complex ion bulk flows in the near-Earth plasma sheet (NEPS) (e.g., Duan et al., 2008; Liang et al., 2009). Especially, it is more complex in the inner edge of NEPS. Usually, the substorm-associated dipolarizations in the NEPS are accompanied with earthward ion bulk flows (e.g., Angelopoulos et al., 1992; Baumjohann et al., 1999; Duan et al., 2011; Liang et al., 2009; Liu et al., 2008; Nakamura et al., 2009; Shiokawa et al., 1998). Using the conjunction observations of the Time History of Events and Macroscale Interactions during Substorms (THEMIS) multiple probes in the NEPS, Duan et al. (2011) pointed out that the dipolarization at inner edge of the near-Earth plasma sheet had no one-to-one relationship with the earthward ion bulk flow. Lui et al. (1999) pointed out

that dipolarization at $X \sim 10\,R_E$ was detected with tailward flows. Inside geosynchronous orbit, magnetic dipolarizations were detected with the earthward ion bulk flow (Dai et al., 2015).

Near-Earth dipolarizations with low-frequency waves are detected with thermal ions and electron energization (e.g., Dai et al., 2015; Liang et al., 2009; Nosé et al., 2014; Ohtani et al., 2018). These energetic particles are the main source of inner magnetosphere during substorms and storms. Nosé et al. (2014) proposed that the dipolarizations associated with low-frequency fluctuations were observed in the inner magnetosphere during the storm main phase. These low-frequency electromagnetic waves can accelerate O^+ ions in the perpendicular direction. The low-frequency waves can accelerate particles crossing the magnetic field with a large perpendicular electric field (e.g., Dai et al., 2014, 2015; Duan et al., 2016; Nosé et al., 2014). Usually, dipolarization associated dispersionless energetic particle injections are accompanied with earthward ion bulk flows in the NEPS (Dai et al., 2015). But few reports show dipolarizations with a sharp increase in the energy flux of energetic particles are associated with tailward ion flows at or inside geosynchronous orbit.

The ballooning mode which occurred in the near-Earth plasma sheet is associated with a tailward expansion of the plasma sheet during substorms (Liu, 1997; Liu et al., 2008; Liu and Liang, 2009; Liang et al., 2009; Saito et al., 2008). Liu et al. (2008) pointed out that the ballooning mode could excite a quasi-electrostatic field a few minutes before local current disruption and that the perturbations associated with the ballooning instability propagated downtail.

In this paper we present dipolarizations with tailward ion flows inside geosynchronous orbit during an intense substorm expansion phase. The observations of an intense substorm on 27 August 2014 by THEMIS-D (TH-D) and THEMIS-E (TH-E) are presented in detail in Sect. 2. Discussions and conclusions of our observations are displayed in the last section.

2 Observations of an intense substorm on 27 August 2014

The OMNI data of the solar wind, interplanetary magnetic field (IMF) and the Disturbance Storm Time (Dst) and AE geomagnetic field indices, during a storm on 27 August 2014, are presented in Fig. 1. The minimum value of SYM-H index is about −90 nT, as shown in Fig. 1f and implies that a moderate storm had taken place. During the main phase of this moderate storm, there was an intense substorm with the AE maximum value 700 nT around 10:10 UT. The beginning of this intense substorm expansion phase was around 09:31 UT with decrease in AL index. A significant substorm enhancement occurred around 09:48 UT with a sharp decrease in AL index and an increase in AE index.

During this intense substorm, THEMIS probes (Angelopoulos, 2008) TH-D and TH-E were both located in the near-Earth magnetotail. Figure 2 displays the orbits of TH-D and TH-E from 09:20 to 10:00 UT in the solar magnetic (SM) coordinate system. At 09:30 UT, locations of these two spacecraft in SM coordinates were (−6.10, −0.06, 0.43) R_E for TH-D and (−8.26, −2.28, 0.99) R_E for TH-E, respectively. The TH-D orbit plot shows that it was located inside geosynchronous orbit at the beginning of this intense substorm expansion phase. On the other hand, TH-E was located outside geosynchronous orbit. These two spacecraft presented good conjunction observations during this intense substorm expansion phase. The instruments adopted in our investigations were a fluxgate magnetometer (FGM) (Auster et al., 2008), an electrostatic analyzer (ESA) (McFadden et al., 2008), an electric field instrument (EFI) (Bonnell et al., 2008) and a solid state telescope (SST) on-board the THEMIS probes.

Figure 3 shows the plasma parameters and the electromagnetic field detected by TH-D mostly inside geosynchronous orbit at around midnight in the interval from 09:25 to 09:55 UT. The solar magnetic (SM) coordinate system is adopted. The panels from top to bottom represent the following: the total magnetic field value B_t and the B_x component; the B_y and B_z components; the magnetic field elevation angle defined by $\theta = \tan^{-1}(B_z/(B_x^2 + B_y^2)^{1/2})$; the ion and electron density and temperature; the plasma value β ($\beta = 2\mu_0 \mathrm{nT}/B^2$) which determines the location of the satellite (Miyashita et al., 2000); three components of ion bulk flow velocity parallel (black line) and perpendicular (red line) to the magnetic field, V_x, V_y and V_z; three components of the electric field, E_x (red), E_y (black) and E_z (blue); three components of convection electric field from $-\boldsymbol{V} \times \boldsymbol{B}$, E_{cx} (red), E_{cy} (black) and E_{cz} (blue), respectively. Figure 3 displays the distinct fluctuations of the magnetic field and plasma density and velocity at around 09:30 and 09:36 UT, respectively. The magnetic elevation angle has two step enhancements as displayed in Fig. 3c. The first increase in elevation angle is from about 15 to 25° during the interval from 09:30:34 to 09:30:54 UT, which are marked by the left two vertical dashed lines in Fig. 3. The total magnetic field value and the B_x component both decrease. The B_z component increases weakly from about 35 to 45 nT. The B_y component has obvious fluctuations around 0 nT. These magnetic signatures indicate a magnetic dipolarization had taken place inside geosynchronous orbit around (−6.10, −0.06, 0.43) R_E. During this weak magnetic field dipolarization, the plasma beta value, β, increases from around 0.5 to 1.0. The electron density and temperature both increase. The ion density also increases, but the ion temperature decreases. This dipolarization accompanied by tailward ion bulk flows, $V_{//x} \sim -100\,\mathrm{km\,s^{-1}}$, and the perpendicular component to the magnetic field in the X direction, $V_{\perp x} \sim -50\,\mathrm{km\,s^{-1}}$, is detected by TH-D, as shown in Fig. 3g. The perpendicular velocity in the Y direction is mainly dawnward at the beginning of this dipo-

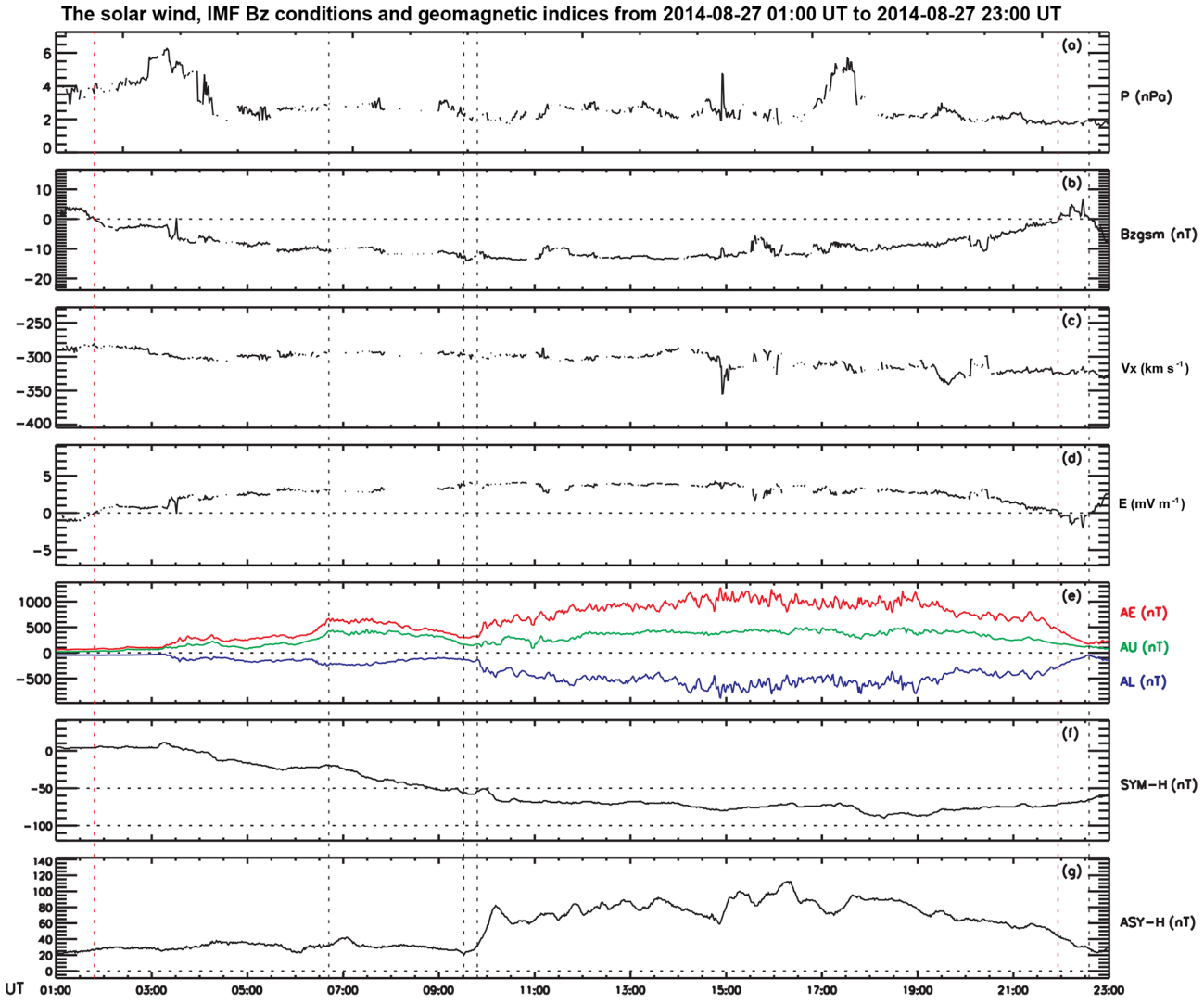

Figure 1. The solar wind, IMF B_z conditions and geomagnetic indices between 01:00 and 23:00 UT on 27 August 2014. From top to bottom, panels **(a–g)** show the change of solar wind dynamic pressure **(a)**, $B_{z,\mathrm{IMF}}$ in geocentric solar magnetospheric (GSM) coordinates **(b)**, the x component of the solar wind flow speed in GSM coordinates **(c)**, electric field E **(d)**, AE–AU–AL indices **(e)**, SYM-H index **(f)** and ASY-H index **(g)**. From left to right, the vertical dotted lines in **(a–g)** panels mark the times 01:48, 06:42, 09:31, 09:48, 21:56 and 22:35 UT, respectively.

larization, $V_{\perp y} \sim -30\,\mathrm{km\,s^{-1}}$. The electric field detected by TH-D also has large fluctuations with negative E_y values during the first depolarization as shown in Fig. 3j. During the intervals from 09:30:34 to 09:30:54 UT, the convection electric field direction is dawnward with a large magnitude, $E_{cy} \sim -12\,\mathrm{mV\,m^{-1}}$, as presented in Fig. 3k. The second magnetic field elevation angle increases sharply at around 09:36 as displayed in Fig. 3c marked by the right two vertical dashed lines. The elevation angle increases from about 25 to 45° during the interval from 09:36:06 to 09:36:21 UT. The magnetic field has similar variations to the first dipolarization signatures. Especially, the second dipolarization has larger elevation angle maximum value, ∼ 45°, as marked by the fourth vertical dashed line in Fig. 3c. During the second dipolarization, the tailward ion bulk flows perpendicular to the magnetic field is also detected by TH-D, $V_{\perp x} \sim -70\,\mathrm{km\,s^{-1}}$, as presented in Fig. 3g. Also the significant negative E_y component is accompanied by this intense dipolarization in Fig. 3j and k.

During the intervals of magnetic dipolarizations with tailward ion bulk flows detected by TH-D inside geosynchronous orbit, TH-E observed a very weak increase in the magnetic field elevation angle and the B_z component around 09:35 and 09:41 UT, as shown in Fig. 4b and c, about 5 min after the two dipolarizations detected by TH-D. The ion and electron densities and temperature increase weakly from very low values as displayed in Fig. 4d and e. Outside geosynchronous orbit, TH-E observed very low beta values, as

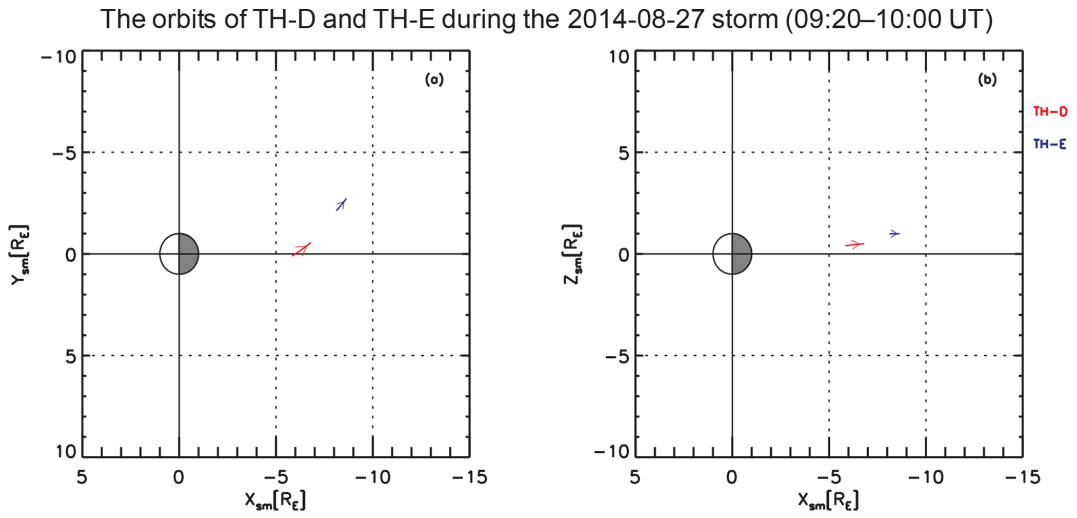

Figure 2. The orbits of TH-D and TH-E in the $X - Y_{\mathrm{SM}}$ plane and the $X - Z_{\mathrm{SM}}$ plane from 09:20 to 10:00 UT on 27 August 2014, which were in the nightside magnetosphere. The arrow shows the flying direction of the satellites. TH-D is red and TH-E is blue.

shown in Fig. 4f, $\beta \sim 0.01$ and $\beta \sim 0.2$ around 09:35 and 09:41 UT, respectively. An interesting phenomenon, where the weak dipolarization was with tailward ion bulk flows, $V_{//x} \sim -180\,\mathrm{km\,s^{-1}}$, was also detected by TH-E around 09:35 UT, as shown in Fig. 4g. The perpendicular velocity is dominated in the negative Y direction, $V_{\perp y} \sim -50\,\mathrm{km\,s^{-1}}$.

The energy fluxes of energetic electrons associated with the intense electric field inside geosynchronous orbit during the two dipolarizations, as shown in the middle panel of Fig. 5, with energies of 31 (blue), 41 (gray), 52 (red), 65.5 (black), 93 (brown) and 139 keV (purple), all simultaneously increase at 09:30:38 and 09:36:09 UT as detected by the SST on-board TH-D. These energetic electrons have a quasi-perpendicular pitch angle distribution, as presented in the bottom panel of Fig. 5.

3 Discussion and conclusions

The dipolarizations with tailward ion bulk flows inside geosynchronous orbit are investigated in our present paper. The energy fluxes of energetic electrons accompanied these dipolarizations with energies between 31 and 139 keV simultaneously increase inside geosynchronous orbit. In accordance with these energetic electron pitch angle distributions, it was found that high-energy electrons were mainly in the quasi-perpendicular direction to the magnetic field, as shown in Fig. 5. On the other hand, the inductive electric field during these two magnetic dipolarizations was in the dawnward direction as displayed in Fig. 3j and k. Previous research work reported that the inductive electric field associated with substorm dipolarization can accelerate particles in the near-Earth plasma sheet (e.g., Dai et al., 2014, 2015; Duan et al., 2016; Fu et al., 2011; Fok et al., 2001; Liu et al., 2010; Lui et al., 1988, 1999; Nakamura et al., 2009; Nosé et al., 2014). As shown in Fig. 3j, at around 09:36:30 UT the inductive electric fields in the second dipolarization are dominated in the E_y component with a large negative value, $E_y \sim -25\,\mathrm{mV\,m^{-1}}$, and the X component also increases with a negative value $E_x \sim -6\,\mathrm{mV\,m^{-1}}$. This intense electric field can drive ions moving into the tailward–dawnward direction. On the other hand, we can calculate the energy quantity relationship between the electric field and energetic electrons. The energy of such an intense E_y in the distance of ~ 1000 km is about $\sim 10^{-15}$ J. The energetic electrons with energy range from 31 to 139 keV are of the same energy order $\sim 10^{-15}$ J. It is inferred that the intense E_y can perpendicularly accelerate electrons to a state of tens of kiloelectronvolts.

Dipolarizations occurring at the inner edge of plasma sheet are complicated with disturbances of ion bulk flows and the electromagnetic field. Lui et al. (1999) pointed out that near-Earth dipolarization was a non-magnetohydrodynamic (non-MHD) process and was also accompanied with tailward ion flows. Our observations of dipolarizations inside geosynchronous orbit are also associated with tailward ion flows. This result is consistent with the report proposed by Liu et al. (2008) that the perturbations associated with the ballooning mode in the near-Earth plasma sheet propagate tailward. Based on the statistical studies, Nosé et al. (2016) proposed that the occurrence probability of the dipolarizations in the inner magnetosphere had a peak at 21:00–00:00 magnetic local time (MLT). Our observations show that two distinct dipolarizations with tailward flows inside geosynchronous orbit are detected by TH-D around 00:02 and 00:05 MLT, respectively.

According to the distance between TH-D and TH-E, $(-2.23, -2.30, 0.56\,R_{\mathrm{E}})$ and the delay time of dipolarization from inside to outside geosynchronous orbit, ~ 5 min, the dipolarization propagating speeds or the plasma sheet ex-

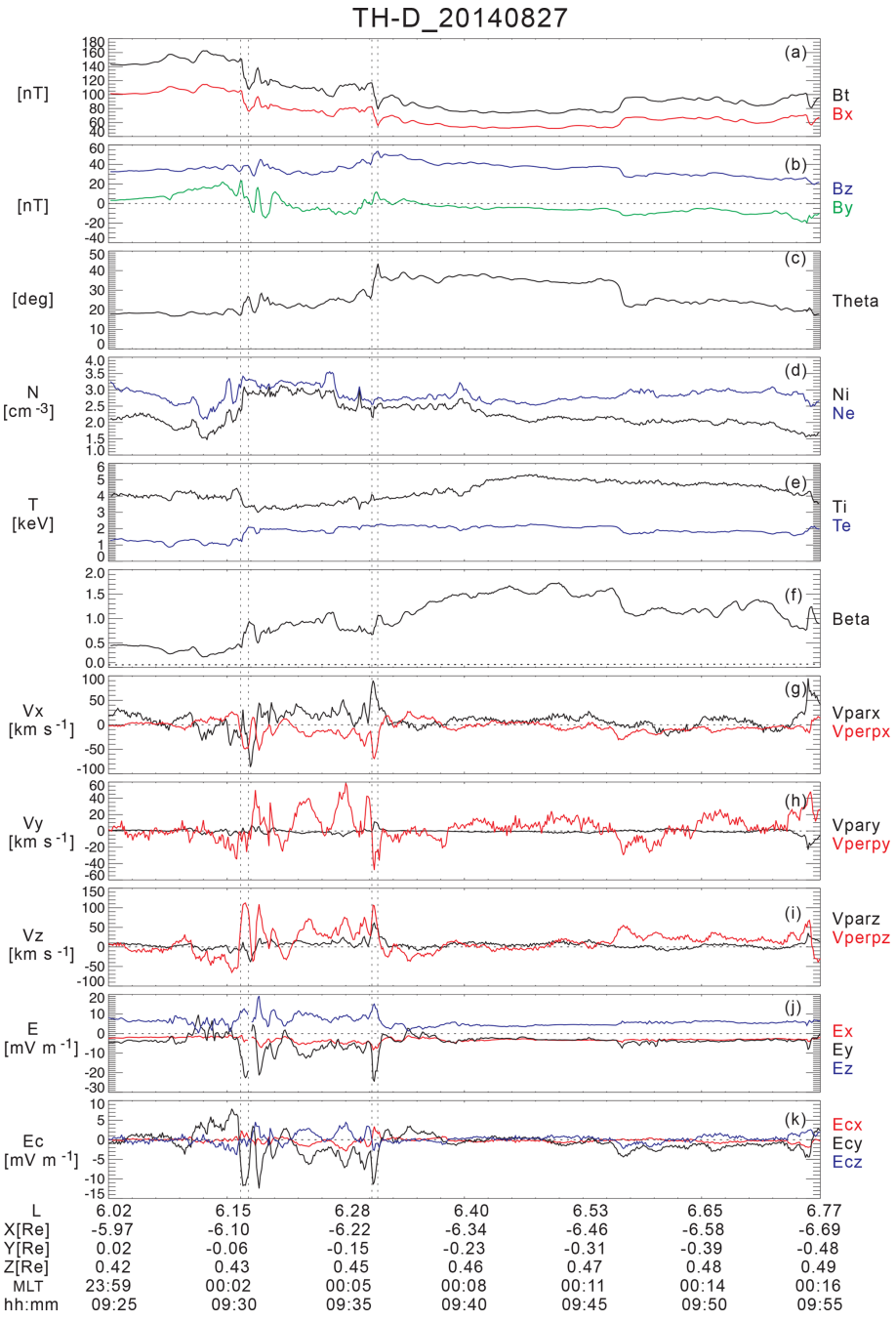

Figure 3. The electromagnetic field and plasma parameters detected by TH-D in intervals from 09:25 to 09:55 UT on 27 August 2014. The solar magnetic (SM) coordinate system is adopted. From top to bottom, panels show **(a)** the total magnetic field B_t (black) and the X component B_x (red), **(b)** the Y component B_y (green) and the Z component B_z (blue), **(c)** the magnetic field elevation angle θ; **(d)** ion and electron density N_i, N_e, **(e)** ion and electron temperature T_i, T_e, **(f)** plasma beta β, **(g)** the X component of ion parallel velocity and perpendicular velocity V_{parx}, V_{perpx}, **(h)** the Y component of ion parallel velocity and perpendicular velocity V_{pary}, V_{perpy}; **(i)** the Z component of ion parallel velocity and perpendicular velocity V_{parz}, V_{perpz}, **(j)** the electric field E_x (red), E_y (black) and E_z (blue) by assuming $\boldsymbol{E} \times \boldsymbol{B} = 0$ and **(k)** the electric field E_{cx} (red), E_{cy} (black), E_{cz} (blue) calculated by $\boldsymbol{E} = \boldsymbol{B} \times V$. The black vertical dashed lines mark the times 09:30:34, 09:30:54, 09:36:06 and 09:36:21 UT, respectively.

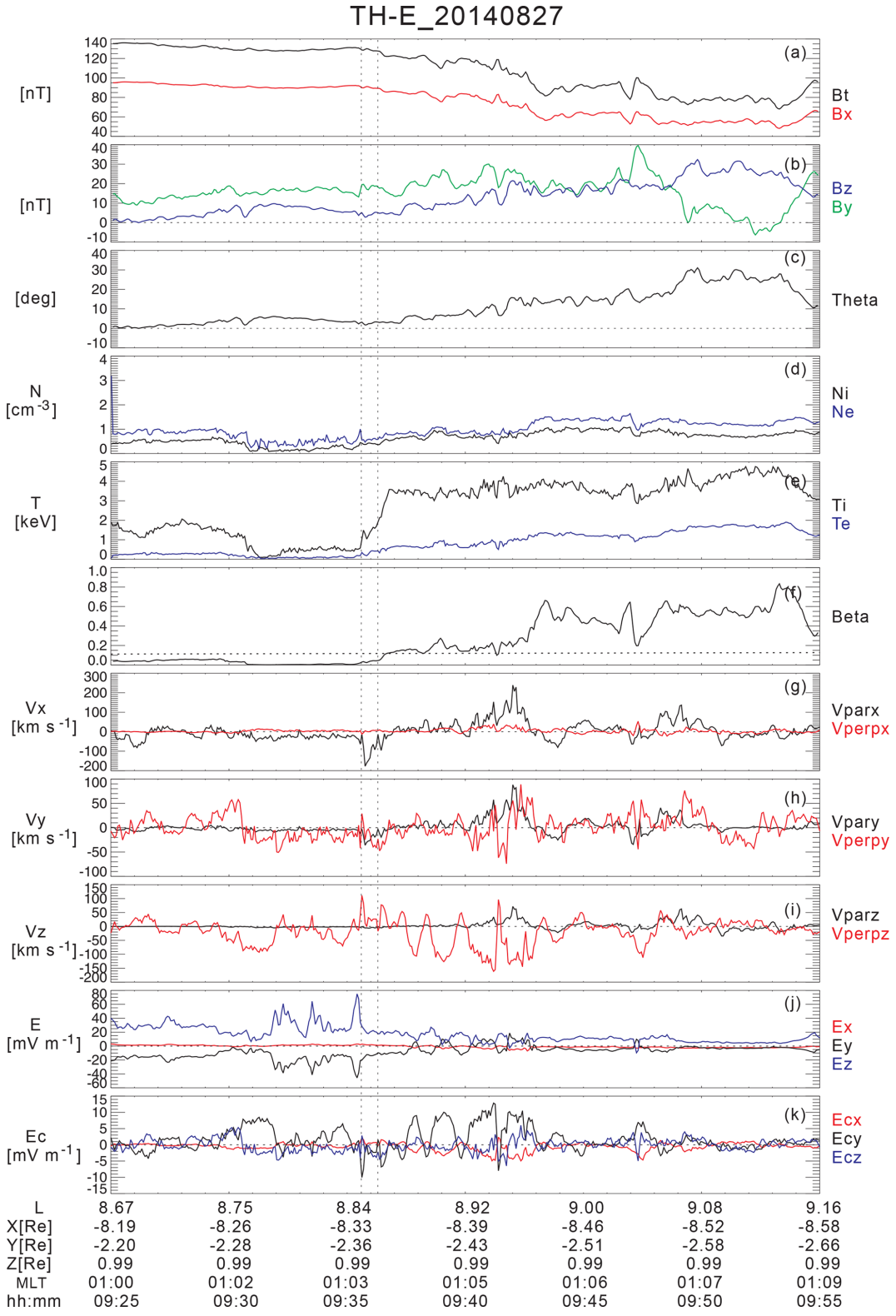

Figure 4. The electromagnetic field and plasma parameters detected by TH-E in intervals from 09:25 to 09:55 UT on 27 August 2014. The figure format is the same as Fig. 3. The black vertical dashed lines mark the times 09:35:36 and 09:36:18 UT.

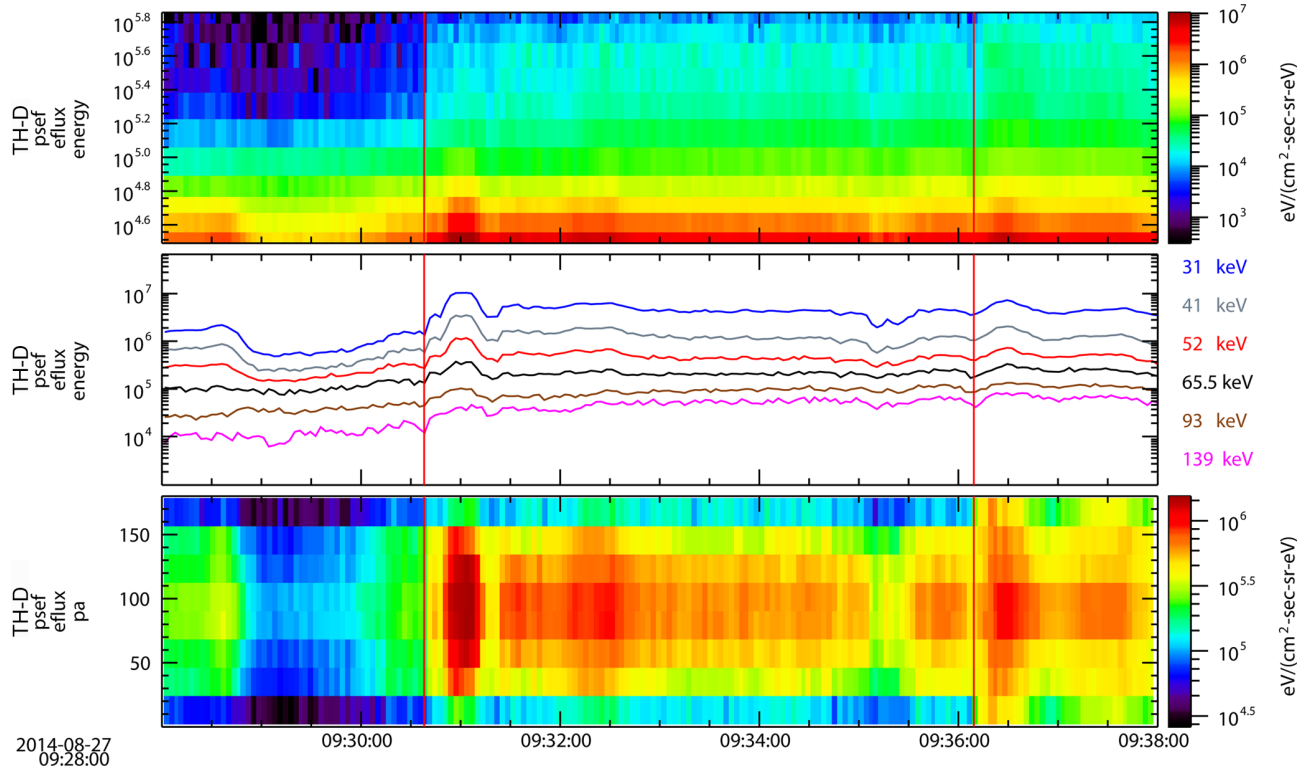

Figure 5. The energetic electrons energy flux (psef) and pitch angle (pa) distribution of energetic electrons detected by the SST on-board TH-D in 3 s time resolution. The red vertical lines mark the times 09:30:38 and 09:36:09 UT.

panding speeds can be estimated as $V_x \sim -47$, $V_y \sim -48$ and $V_z \sim 12\,\mathrm{km\,s^{-1}}$, respectively. Liou et al. (2002) proposed that the dipolarization region expanding speed was $\sim 60\,\mathrm{km\,s^{-1}}$ westward at geosynchronous orbit. By comparing observations between TH-D and TH-E in our investigations, the azimuth speed of dipolarization region is obtained $\sim 48\,\mathrm{km\,s^{-1}}$. These two observational results are consistent with each other. The dipolarization associated with the current disruption propagated tailward with a speed of $V_x \sim -100\,\mathrm{km\,s^{-1}}$ detected by THEMIS satellites in the near-Earth plasma sheet $X \sim -11\,R_\mathrm{E}$ (Liu et al., 2008). It is larger than the dipolarization propagating speed from inside to outside geosynchronous orbit $V_x \sim -47\,\mathrm{km\,s^{-1}}$. The different speeds of dipolarizations propagating tailward imply that the magnitude of the dipolarization speed may be associated with its beginning location in magnetotail plasma sheet.

On the other hand, Lui (1991) reported that substorm disturbance propagated tailward through a rarefaction wave front accompanied by earthward flows during the early substorm expansion phase period. Chao et al. (1977) proposed that the rarefaction wave propagating tailward was accompanied by the thinning of the plasma sheet and an earthward plasma flow. This earthward flow is possibly a convection flow or outflow of magnetic reconnection from the middle magnetotail.

Based on the above observation analysis, we can draw the results as follows. Two distinct magnetic dipolarizations with tailward ion flows are observed by TH-D inside geosynchronous orbit on 27 August 2014 during the intense substorm with $\mathrm{AE_{max}} \sim 1000\,\mathrm{nT}$. TH-D was located inside geosynchronous orbit around midnight in the interval from 09:20 to 10:00 UT. The first dipolarization is displayed by the magnetic elevation angle increase from 15 to 25° around 09:30:40 UT. The second one is presented by the elevation angle increase from 25 to 45° around 09:36 UT. These two significant dipolarizations are accompanied by the energy flux of energetic electrons which simultaneously increase inside geosynchronous orbit. After a 5 min expansion tailward of near-Earth plasma sheet, TH-E located outside geosynchronous orbit also detects this tailward expanding plasma sheet with an ion flow of $-150\,\mathrm{km\,s^{-1}}$. The dipolarization propagates tailward with a speed of $-45\,\mathrm{km\,s^{-1}}$ along a $2R_\mathrm{E}$ distance in the X direction between TH-D and TH-E within 5 min. These dipolarizations with tailward ion flows observed inside geosynchronous orbit indicate a new energy transfer path in the inner magnetosphere during substorms.

Data availability. The OMNI data of the solar wind, interplanetary magnetic field (IMF), and SYM-H, AE, AU and AL geomagnetic field indices are freely available from the Space Physics Data Facil-

ity (SPDF) at https://omniweb.gsfc.nasa.gov/form/omni_min.html (NASA's GSFC, Goddard Space Flight Center, last access: 11 June 2018). THEMIS data of the electromagnetic field and plasma parameters are publicly available from NASA at http://themis.ssl.berkeley.edu/data/themis/ (NASA, last access: 13 November 2018).

Competing interests. The authors declare that they have no conflict of interest.

Acknowledgements. We acknowledge NASA contract NAS5-02099 for the use of the data from the THEMIS mission. Specifically, we thank Davin E. Larson for the use of the SST data, Charles W. Carlson and James P. McFadden for use of the ESA data, John W. Bonnell and Forrest S. Mozer for use of the EFI data, and Karl-Heinz Glassmeier, Hans-Ulrich Auster and Wolfgang Baumjohann for the use of FGM data provided under the lead of the Technical University of Braunschweig, with financial support from the German Ministry for Economy and Technology and the German Center for Aviation and Space (DLR) under the contract 50 OC 0302. The authors thank NASA CDAWeb and Taiwan Ascii and ldl_save Data Archives (AIDA) for the THEMIS data. The SYM-H index was provided by Data Analysis Center for Geomagnetism and Space Magnetism in Kyoto, Japan. This work is supported by the National Natural Science Foundation of China grants 41674167, 41731070 and 41574161 and in part by the Specialized Research Fund for State Key Laboratories.

Review statement. This paper was edited by Anna Milillo and reviewed by one anonymous referee.

References

Angelopoulos, V.: The THEMIS Mission, Space Sci. Rev., 141, 5–34, 2008.

Angelopoulos, V., Baumjohann, W., Kennel, C. F., Coroniti, F. V., Kivelson, M. G., Pellat, R., Walker, R. J., Lühr, H., and Paschmann, G.: Bursty bulk flows in the inner central plasma sheet, J. Geophys. Res., 97, 4027, https://doi.org/10.1029/91JA02701, 1992.

Auster, H. U., Glassmeier, K. H., Magnes, W., Aydogar, O., Baumjohann, W., Constantinescu, D., Fischer, D., Fornacon, K. H., Georgescu, E., Harvey, P., Hillenmaier, O., Kroth, R., Ludlam, M., Narita, Y., Nakamura, R., Okrafka, K., Plaschke, F., Richter, I., Schwarzl, H., Stoll, B., Valavanoglou, A., and Wiedemann, M.: The THEMIS Fluxgate Magnetometer, Space Sci. Rev., 141, 235–264, 2008.

Baumjohann, W., Hesse, M., Kokubun, S., Mukai, T., Nagai, T., and Petrukovich, A. A.: Substorm dipolarization and recovery, J. Geophys. Res.-Space, 104, 24995–25000, 1999.

Bonnell, J. W., Mozer, F. S., Delory, G. T., Hull, A. J., Ergun, R. E., Cully, C. M., Angelopoulos, V., and Harvey, P. R.: The Electric Field Instrument (EFI) for THEMIS, Space Sci. Rev., 141, 303–341, 2008.

Chao, J. K., Kan, J. R., Lui, A. T. Y., and Akasofu, S.-I.: A model for thinning of the plasma sheet, Planet. Space Sci., 25, 703–710, 1977.

Dai, L., Wygant, J. R., Cattell, C. A., Thaller, S., Kersten, K., Breneman, A., Tang, X., Friedel, R. H., Claudepierre, S. G., and Tao, X.: Evidence for injection of relativistic electrons into the Earth's outer radiation belt via intense substorm electric fields, Geophys. Res. Lett., 41, 1133–1141, 2014.

Dai, L., Wang, C., Duan, S., He, Z., Wygant, J. R., Cattell, C. A., Tao, X., Su, Z., Kletzing, C., Baker, D. N., Li, X., Malaspina, D., Blake, J. B., Fennell, J., Claudepierre, S., Turner, D. L., Reeves, G. D., Funsten, H. O., Spence, H. E., Angelopoulos, V., Fruehauff, D., Chen, L., Thaller, S., Breneman, A., and Tang, X.: Near-Earth injection of MeV electrons associated with intense dipolarization electric fields: Van Allen Probes observations, Geophys. Res. Lett., 42, 6170–6179, 2015.

Duan, S., Liu, Z., Cao, J., Lu, L., Rème, H., Dandouras, I., and Carr, C. M.: TC-1 observation of ion high-speed flow reversal in the near-Earth plasma sheet during substorm, Sci. China Ser. E, 51, 1721–1730, 2008.

Duan, S. P., Liu, Z. X., Liang, J., Zhang, Y. C., and Chen, T.: Multiple magnetic dipolarizations observed by THEMIS during a substorm, Ann. Geophys., 29, 331–339, https://doi.org/10.5194/angeo-29-331-2011, 2011.

Duan, S. P., Dai, L., Wang, C., Liang, J., Lui, A. T. Y., Chen, L. J., He, Z. H., Zhang, Y. C., and Angelopoulos, V.: Evidence of kinetic Alfven eigenmode in the near-Earth magnetotail during substorm expansion phase, J. Geophys. Res.-Space, 121, 4316–4330, 2016.

Fok, M.-C., Moore, T. E., and Spjeldvik, W. N.: Rapid enhancement of radiation belt electron fluxes due to substorm dipolarization of the geomagnetic field, J. Geophys. Res.-Space, 106, 3873–3881, 2001.

Fu, H. S., Khotyaintsev, Y. V., André, M., and Vaivads, A.: Fermi and betatron acceleration of suprathermal electrons behind dipolarization fronts, Geophys. Res. Lett., 38, L16104, https://doi.org/10.1029/2011GL048528, 2011.

Liang, J., Liu, W. W., and Donovan, E. F.: Ion temperature drop and quasi-electrostatic electric field at the current sheet boundary minutes prior to the local current disruption, J. Geophys. Res.-Space, 114, A10215, https://doi.org/10.1029/2009JA014357, 2009.

Liou, K., Meng, C.-I., Lui, A. T. Y., Newell, P. T., and Wing, S.: Magnetic dipolarization with substorm expansion onset, J. Geophys. Res., 107, 1131, https://doi.org/10.1029/2001JA000179, 2002.

Liu, W. W.: Physics of the explosive growth phase: Ballooning instability revisited, J. Geophys. Res.-Space, 102, 4927–4931, 1997.

Liu, W. W. and Liang, J.: Disruption of magnetospheric current sheet by quasi-electrostatic field, Ann. Geophys., 27, 1941–1950, https://doi.org/10.5194/angeo-27-1941-2009, 2009.

Liu, W. W., Liang, J., and Donovan, E. F.: Electrostatic field and ion temperature drop in thin current sheets: A theory, J. Geophys. Res.-Space, 115, A03211, https://doi.org/10.1029/2009JA014359, 2010.

Liu, W. W., Liang, J., and Donovan, E. F.: Interaction between kinetic ballooning perturbation and thin current sheet: Quasi-electrostatic field, local onset, and

global characteristics, Geophys. Res. Lett., 35, L20107, https://doi.org/10.1029/2008GL035757, 2008.

Lui, A. T. Y.: A synthesis of magnetospheric substorm models, J. Geophys. Res., 96, 1849–1856, https://doi.org/10.1029/90JA02430, 1991.

Lui, A. T. Y., Lopez, R. E., Krimigis, S. M., McEntire, R. W., Zanetti, L. J., and Potemra, T. A.: A case study of magnetotail current sheet disruption and diversion, Geophys. Res. Lett., 15, 721–724, 1988.

Lui, A. T. Y., Liou, K., Nosé, M., Ohtani, S., Williams, D. J., Mukai, T., Tsuruda, K., and Kokubun, S.: Near-Earth dipolarization: Evidence for a non-MHD process, Geophys. Res. Lett., 26, 2905–2908, 1999.

McFadden, J. P., Carlson, C. W., Larson, D., Ludlam, M., Abiad, R., Elliott, B., Turin, P., Marckwordt, M., and Angelopoulos, V.: The THEMIS ESA Plasma Instrument and In-flight Calibration, Space Sci. Rev., 141, 277–302, 2008.

Miyashita, Y., Machida, S., Mukai, T., Saito, Y., Tsuruda, K., Hayakawa, H., and Sutcliffe, P. R.: A statistical study of variations in the near and middistant magnetotail associated with substorm onsets: GEOTAIL observations, J. Geophys. Res.-Space, 105, 15913–15930, 2000.

Nagai, T.: Observed magnetic substorm signatures at synchronous altitude, J. Geophys. Res., 87, 4405–4417, https://doi.org/10.1029/JA087iA06p04405, 1982.

Nakamura, R., Retino, A., Baumjohann, W., Volwerk, M., Erkaev, N., Klecker, B., Lucek, E. A., Dandouras, I., Andre, M., and Khotyaintsev, Y.: Evolution of dipolarization in the near-Earth current sheet induced by Earthward rapid flux transport, Ann. Geophys., 27, 1743–1754, 2009.

NASA: THEMIS data of the electromagnetic field and plasma parameters, available at: http://themis.ssl.berkeley.edu/data/themis/, last access: 13 November 2018.

NASA's GSFC: the Space Physics Data Facility (SPDF), available at: https://omniweb.gsfc.nasa.gov/form/omni_min.html, last access: 11 June 2018.

Nosé, M., Takahashi, K., Keika, K., Kistler, L. M., Koga, K., Koshiishi, H., Matsumoto, H., Shoji, M., Miyashita, Y., and Nomura, R.: Magnetic fluctuations embedded in dipolarization inside geosynchronous orbit and their associated selective acceleration of O^+ ions, J. Geophys. Res.-Space, 119, 4639–4655, 2014.

Nosé, M., Keika, K., Kletzing, C. A., Spence, H. E., Smith, C. W., MacDowall, R. J., Reeves, G. D., Larsen, B. A., and Mitchell, D. G.: Van Allen Probes observations of magnetic field dipolarization and its associated O^+ flux variations in the inner magnetosphere at $L<6.6$, J. Geophys. Res.-Space, 121, 7572–7589, 2016.

Ohtani, S., Motoba, T., Gkioulidou, M., Takahashi, K., and Singer, H. J.: Spatial Development of the Dipolarization Region in the Inner Magnetosphere, J. Geophys. Res.-Space, 123, 5452–5463, 2018.

Saito, M. H., Miyashita, Y., Fujimoto, M., Shinohara, I., Saito, Y., Liou, K., and Mukai, T.: Ballooning mode waves prior to substorm-associated dipolarizations: Geotail observations, Geophys. Res. Lett., 35, L07103, https://doi.org/10.1029/2008GL033269, 2008.

Shiokawa, K., Baumjohann, W., Haerendel, G., Paschmann, G., Fennell, J. F., Friis-Christensen, E., Lühr, H., Reeves, G. D., Russell, C. T., Sutcliffe, P. R., and Takahashi, K.: High-speed ion flow, substorm current wedge, and multiple Pi 2 pulsations, J. Geophys. Res.-Space, 103, 4491–4507, 1998.